Comparison between Torsional Spring Constants of Rectangular and V-shaped AFM Cantilevers

Feodor M. Borodich, Raheem S. Al-Musawi, Emmanuel B. Brousseau and Sam L. Evans

***Abstract*—The properties of force-sensing micro-cantilevers are of fundamental importance for measurements employing atomic force microscopy (AFM) techniques. Due to the well-known arguments of Sader, it is generally accepted that V-shaped cantilevers are more sensitive to lateral forces than rectangular ones. We present results of numerical (finite element modelling) and experimental comparison between torsional spring constants of rectangular and V-shaped commercial AFM cantilevers. As representative example of such beams, we considered AFM probes available commercially. In particular, we tested scaled-up models of V-shaped cantilevers which had the same geometrical shapes as commercial AFM cantilevers. Both the rectangular and the V-shaped larger scale models were made of the same material; they had the same length, thickness, normal spring constant, as well as the same location and shape of the tip base. In the experiments and the simulations, an external lateral load was applied to the free end of the tip. A good agreement between the experimental work and finite element method (FEM) simulations was observed. The results show that the torsional spring constant of the V-shape cantilevers considered here was greater than that of the equivalent rectangular beams by up to 45%. The discrepancy with the results from Sader should be caused by differences in both the load transfer scheme and the geometrical shapes of the V-shaped beams.**

***Index Terms*— Atomic force microscope, Frictional force microscope, Torsional spring constant, V-shaped cantilever**

I. Introduction

CURRENT success in the characterization of various surfaces and small objects down to the nanometer scale is, in part, a result of the rapid development of scanning probe microscopy (SPM), and especially the atomic force microscope (AFM). Indeed, AFM instruments have revolutionized the way in which researchers explore micro/nano scale objects today. As was stated by the inventors of the AFM [1], the capability of such instruments to measure inter-atomic scale forces opens the door to a variety of applications. Indeed, the use of AFM allows researchers not only to characterize the structure of sample surfaces [2-4], but also to measure nanometer-scale frictional properties [5,6], to tailor surface nanostructures, via AFM tip-based nanomachining for instance [7], and to manipulate objects at the micro/nano scale [8,9]. AFM tests are also actively used in various other areas, including applications to biological objects [10,11]. Here, we focus on AFM applications involving lateral forces, i.e. manipulation of objects or tests when an AFM works as a frictional force microscope (FFM).

The interaction force between the AFM tip and a sample may be calculated by multiplying the spring constant of the cantilever and its displacement. Hence, the normal and torsional spring constants of force-sensing micro-cantilevers are of fundamental importance for accurate force measurements employing AFM techniques. It is known that the torsional spring constant of a FFM should be minimized in order to make the cantilever sensitive to the lateral forces [12]. Due to the well-known arguments of Sader [13,14], it is generally accepted that V-shaped cantilevers are more sensitive to lateral forces than rectangular ones. Here we present results of numerical (finite element modelling) and experimental comparison between torsional spring constants of rectangular and V-shaped AFM cantilevers that were made of the same material and having same length, thickness, normal spring constant, as well as identical location and shape of the tip base. The geometrical shapes of the V-type cantilevers studied were the same as the shapes of some commercial AFM cantilevers. As representative examples of such beams, we considered the AFM cantilevers provided by Olympus, namely the cantilevers of the OMCL-TR series. It is shown that the torsional spring constant of V-shaped cantilever samples is greater than the constant of the rectangular beam by up to 45% depending on the specific geometry of the cantilever. We argue that the results of the Sader experiments [13,14] do not necessarily apply for interpretation of work of all commercial AFM cantilevers. The discrepancy of outcomes should be caused by the differences in the load transfer scheme and the geometrical shapes of the used V-shaped models.

The paper is organized as follows. In section 2, we present a preliminary discussion related to mechanics of AFM cantilevers. Then, in section 3, we present arguments based on dimensional analysis to support the design choice of the cantilever large scale models used in the adopted experimental

F. M. Borodich is with the School of Engineering, Cardiff University, Cardiff, CF24 3AA, UK (e-mail: BorodichFM@cardiff.ac.uk).

R. S. Al-Musawi, was with Cardiff University, Cardiff, CF24 3AA, UK. He is now with the Department of Mechanical Engineering, University of Kufa, Iraq.

E. B. Brousseau and S. L. Evans are both with the School of Engineering, Cardiff University, Cardiff, CF24 3AA, UK

methodology. In section 4, we present the results of experimental studies and numerical simulations by the finite element method (FEM) of laterally loaded cantilevers. In particular, we present results that enable us to compare the torsional spring constants between equivalent rectangular and V-shaped cantilevers. As has been mentioned, the scaled-up models of V-shaped cantilevers tested had the same geometrical shapes as the commercial Olympus AFM cantilevers and the load was transferred to the cantilevers through the four-sided base of the probe.

II. Preliminaries

An AFM probe is a lever usually referred to as a "cantilever" with a tip attached at its free end. The tip is usually a sharp pyramid. To study friction or to manipulate nano-size objects, the probe can interact with a surface in contact mode. To move the probe in a lateral direction in contact mode, one needs to apply not only the normal component of the external load (F_N) but also a tangential force (F_T). The contact interactions will cause corresponding vertical (F_R) and frictional (F_F) reactions of the surface (see Fig. 1a). These forces will create a twisting moment. Hence, to characterize deformations of the cantilever during its lateral motion in contact mode, one needs to take into account its torsional rigidity.

In papers devoted to studies of AFM cantilever beams [2], the axis directed along the beam is usually denoted as x, and the vertical and lateral axes as z and y respectively (see Fig. 1b). These notations are used in most of the leading theoretical papers devoted to studies of lateral stiffness of AFM beams (see, e.g. [6,12,15,16]). However, these notations of axes differ slightly from traditional notations of Strength of Materials [17].

Because the scope of the study is related to the elastic deformation of cantilever beams, the classical Euler-Bernoulli beam theory is applicable (see, e.g. Sarid [18], Bushan and Marti [19], Sánchez Quintanilla [2], along with classical papers on the subject from Butt *et al.* [20], Heim *et al.* [21], Hutter [22], Holbery *et al.* [23], Clifford and Shea [24] and Cannara *et al.* [25], for instance). This is the analytical approach that we also applied in a previous paper dedicated to the normal bending of a rectangular AFM probe in the specific context AFM-based nanomachining [7]. Hence, the classic beam theory can be applied to both scaled-up models and microscale AFM cantilevers provided strains are elastic and the assumption of small deflections and small angles of the beam is not violated.

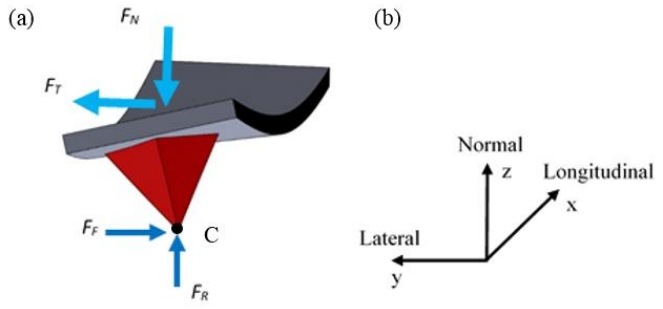

Fig. 1 (a) Schematic of a rectangular AFM cantilever loaded by both normal (F_N) and tangential (F_T) components of external load and corresponding vertical (F_R) and frictional (F_F) reactions. (b) Directions of the Cartesian axes. C denotes the contact point (i.e. the tip apex).

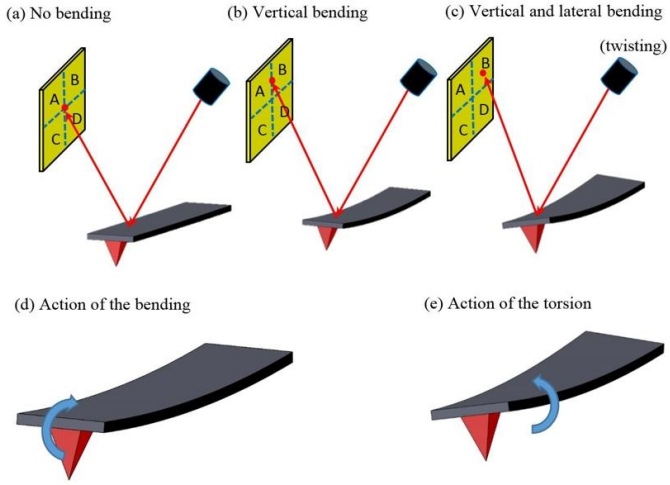

Fig. 2 Positions of the incident spot of the reflected laser beam depending of the cantilever deformations: (a) no bending; (b) vertical bending only; and (c) vertical and lateral bending. The types of external moments caused by both normal (F_N) and tangential (F_T) components of external load applied to the AFM tip: (d) bending due to the normal force (F_N) and corresponding vertical (F_R) reaction; and (e) torsion due to the tangential force (F_T) and corresponding frictional (F_F) reaction.

Contemporary AFMs use optical levers such that a laser beam focused on the free end of the cantilever upper surface is reflected to a section (cell) of a split photodiode (see cells A, B, C and D in Fig. 2a,b,c) or a position sensitive photo detector (PSPD) [2]. If there is no bending or torsion of the cantilever, then the incidence spot of the reflected laser beam is located in the center of the photodiode (Fig. 2a). If the cantilever beam is only under the action of the bending moment (Fig. 2d) then, only the vertical displacement of the reflected laser spot (Fig. 2b) is detected using the signal difference between the upper half and the lower half of the PSPD (also commonly referred to as the 'A-B' output signal). If, in addition to the action of the bending moment, the cantilever is under the action of a torsion moment caused by the tangential force (F_T), with the corresponding frictional (F_F) reaction (Fig. 2e), then the horizontal displacement of the incident spot of the reflected laser beam will be also detected (Fig. 2c).

It will be assumed that the linear description is sufficient to describe the deformation of an AFM cantilever. Then, one can introduce the notion of spring constants (stiffnesses) K_x, K_y, and K_Z of a cantilever that are coefficients of proportionality between the components of the tip displacement and the appropriate loads, i.e.

$$F_N = K_z\,\Delta z,\quad F_T = K_y\,\Delta y, \text{ and } F_x = K_x \Delta x \tag{1}$$

where Δx, Δy, and Δz are the displacements of the AFM tip along the corresponding axes, and F_x, F_T, and F_N are the forces applied to the beam and acting along the axes x, y, and z respectively. We do not consider further the constant K_x because it does not relate to the lateral mode; but rather to the forward and backward contact modes used in AFM tip-based nanomachining. The specific features of the mechanical problem related to this kind of nanomachining have been

recently discussed in detail in a previous paper [7]. One can see (Fig. 1a) that the external force F_T and the frictional force F_F create a couple (a torque T) and hence, it is useful to introduce the torsional spring constant K_θ that connects the torsional deflection angle $\Delta\theta$, and the torque T, as follows:

$$T = K_\theta \, \Delta\theta \tag{2}$$

Torque has physical dimension of force times distance. Indeed, the torque $T = F_F \, h_p$, where h_p is the height of the probe tip. Hence, using the Lagrangian mechanics terminology, one can say that spring constants of a cantilever are coefficients of proportionality between the generalized displacements: Δy and Δz, and the twist angle (the torsional deflection angle) $\Delta\theta$, and the appropriate generalized loads.

If the cantilever beam is rectangular, then the spring constants due to bending of the beam K_y^b and K_Z may be estimated using the Bernoulli-Euler beam theory [17]

$$K_z = \frac{Ewt^3}{4L^3} \tag{3a}$$

and

$$K_y^b = \frac{Etw^3}{4L^3} \tag{3b}$$

where t, w and L are the thickness, width and length of the cantilever respectively and E is the elastic modulus of its material. Usually the width w of an AFM cantilever is about one order of magnitude greater than its thickness t, hence $K_z \ll K_y^b$. We have used the superscript b to indicate that the value is related to bending of the beam in the lateral direction.

Although the elementary Bernoulli-Euler beam theory is applicable to calculate the spring constants K_y^b and K_Z (see (3a) and (3b)), the elementary theory of torsion is not applicable to AFM cantilevers because its elementary equations are valid only to solids having circular cross sections. The problem of twist of bars of rectangular cross sections is complicated due to warping of the cross section during twist [17]. The problem is even more complicated if the cantilever is V-shaped. In fact, the lateral displacement Δy may be represented as $\Delta y = \Delta y^b + \Delta y^t$, where the superscript t indicates that the value is related to the torsion of the beam. Correspondingly, we can write $1/K_y = 1/K_y^t + 1/K_y^b$. Because the value Δy^t is usually much greater than Δy^b, the bending component may be neglected, i.e. it is assumed that $K_y^b = \infty$. Hence, $K_y \cong K_y^t$. In addition, it is clear that the lateral spring constant K_y may be easily re-calculated to the torsional spring constant K_θ in (2). Indeed, $\Delta\theta \cong \Delta y/h_p$ since $\tan\Delta\theta \cong \Delta\theta$ when the torsional deflection angle is small. Hence, it is the same to compare the K_θ or the K_y of cantilevers.

The original AFM was proposed to operate with a rectangular cantilever [1]. However, it was soon suggested by Albrecht and Quate [26] (see also [27]) to use V-shaped micro-cantilevers to increase the lever lateral stiffness (see Fig. 3a and 3b). Baselt and Baldeschwieler [28] provided an experimental comparison of the average lateral deflection signals from rectangular and V-shaped cantilevers of length L=100 μm when scanning the same sample. They estimated that the lateral spring constant which includes both the torsional and the lateral bending modes, is ten times greater for a V-shaped cantilever than for the corresponding rectangular cantilever.

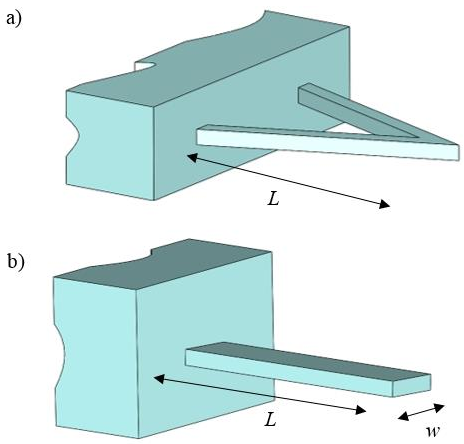

Fig. 3 Schematic of (a) V-shaped and (b) rectangular cantilevers.

In addition, even for rectangular beams, AFM manufacturers cannot fabricate cantilevers with nominal values of spring constants. Hence, cantilevers have to be calibrated before they may be used in AFM applications. The determination of the cantilever spring constants has been a crucial issue in modern nanometrology applications. The related questions have been intensively studied (see, e.g. [6,9,15,24,25,29-33]). These studies of spring constants of AFM cantilevers combine analytical approaches and finite element analysis because no exact analytical solution exists. The analytical studies of V-shaped cantilevers often involve some additional assumptions. For example, it was assumed that two rectangular cantilevers placed parallel to each other are approximately equivalent to one V-shaped cantilever [27]. Further, simplification of the geometrical shapes of the V-shaped AFM cantilevers to some ideal shapes have often been involved in the studies. For example, V-shaped cantilevers have been modelled as a triangular plate having a triangular part of material removed (see Fig. 3a), i.e. a triangular plate connected to two prismatic beams (see, e.g. [13,15]), while the real geometry of

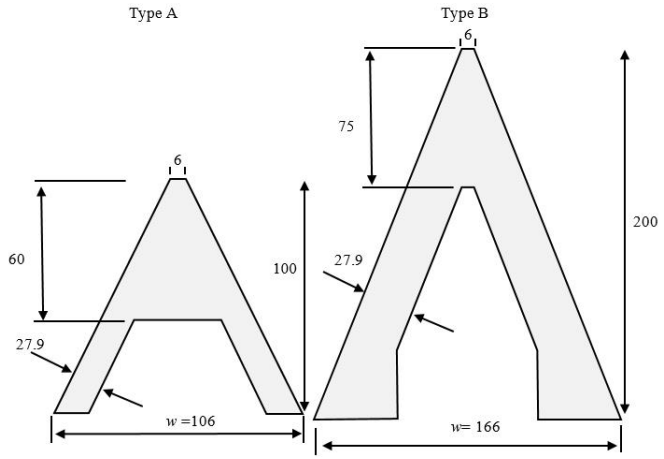

Fig. 4 The real geometry of two Olympus commercial V-shaped cantilevers (types A and B) according to the company description [28]. The thickness of both cantilevers is 0.8. All dimensions are in μm.

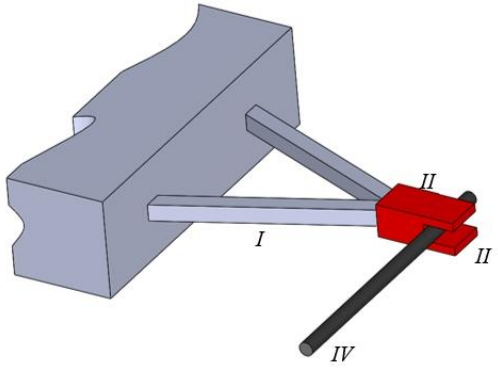

Fig. 5 Schematic of the experimental technique used by Sader and Sader [14] for measuring the torsional spring constant. The cantilever (I) was loaded not through a force applied at the end of a tip but rather through a clamp (II) with an attached rod holder (III) by a moment created by a force applied to the end of an aluminum rod (IV) having the following dimensions: length 1 m and diameter 10 mm.

commercial V-shaped cantilevers is typically more complicated (see Fig. 4).

In 2003, Sader [13] published an analysis of the susceptibility of AFM cantilevers to lateral forces. He presented a detailed comparison of the complementary performance of V-shaped and rectangular cantilevers, with regards to their susceptibility to lateral forces. It is clear from his description that rectangular and V-shaped cantilevers of identical normal stiffness and length were studied. In the analysis, beams having ideal geometry were loaded by external torque (as it is described in Fig. 5). His analysis showed that V-shaped AFM cantilevers were generally more prone to the effects of lateral forces than rectangular AFM cantilevers. These studies were supported by experiments [14]. Fig. 5 describes the large-scale model studied by Sader and Sader [14] and their experimental technique. One can see that although the cantilever was loaded by proper total torque, the forces were applied using an aluminum rod through a clamp and not through the base of the probe attached at the cantilever tip. The dimensions of the used rod were as follows: length of 1 m and a diameter of 10 mm. Although Sader and Sader [14] argued that to examine the resistance of the cantilever to moment loads produced by a lateral force applied via the apex of the imaging tip, one may load the cantilever directly by a torque (Fig. 5), we believe that the results of these studies cannot be used directly to interpret the work of real commercial AFM cantilevers. This is because, in practice, the load is transferred to the beam through the base of the imaging tip, while the load is applied at the tip apex. Thus, we present new experimental procedures that accurately reflect both the geometry of commercial cantilevers and the load transfer scheme used in a real AFM.

III. Experimental Methodology for Cantilever Design

Here the experimental studies are based not on testing the twisting of real AFM cantilevers but on scaled-up models. The experimental methodology employed in our studies, including a description of the scaled cantilever design and the approach used to work with equivalent scaled-up models of rectangular and V-shaped geometry, is described in this section.

A. Geometry of the models

For the experimental analysis of normal and lateral behavior, both rectangular and V-shaped cantilevers were used. Because the V-shaped probes manufactured by Olympus, NanoWorld and other AFM probe manufacturers are quite similar, we took Olympus probes as a representative sample of commercial V-shaped cantilevers. Thus, the V-shaped cantilevers tested were large scale models of types A and B shown in Fig. 4, whose geometry was taken from the company description [34]. According to the specifications given by Olympus, cantilevers of the same types are manufactured with different values of thickness, e.g. $t = 0.8$ μm or 2 μm, keeping the same dimensions for the length and the width. Here, we have taken $t = 0.8$ μm as the basis for the thickness value of the cantilevers. The thickness of the large-scale models, t_M, was taken as 1, 2 and 3 mm. According to the usual procedure of model preparation [35, 36], the models were chosen as geometrically similar to the original prototypes. Hence, all geometrical characteristics of the models can be calculated using the scaling factor Λ_s, defined as:

$$\Lambda_s = \frac{Model\ dimension}{Original\ dimension} \tag{4}$$

Hence, if the sheet thickness of the material used to prepare the large-scale models is t_M=1 mm, then $\Lambda_s = \frac{t_M}{t} = \frac{1000}{0.8} = 1250$, while $\Lambda_s = 2500$ for t_M=2 mm. It is clear that the dimensionless length ($\tilde{L}$) and width ($\tilde{w}$) of the cantilever of the prototypes and models should be the same:

$$\tilde{L} = \frac{L}{t},\ \tilde{w} = \frac{w}{t} \tag{5}$$

In our case, $\tilde{L}_1 = \frac{100}{0.8} = 125$ and $\tilde{w}_1 = \frac{106}{0.8} = 132.5$ and $\tilde{L}_2 = 250$, $\tilde{w}_2 = 207.5$ for cantilevers of types A and B, respectively. Other geometrical characteristics of the models were calculated using (4). For cantilevers of the type A and t_M=2 mm and for cantilevers of the type B and t_M=1 mm , the geometrical values of the width w_M and the length L_M, along with other geometrical characteristics of the large scale models, are shown in Fig. 6.

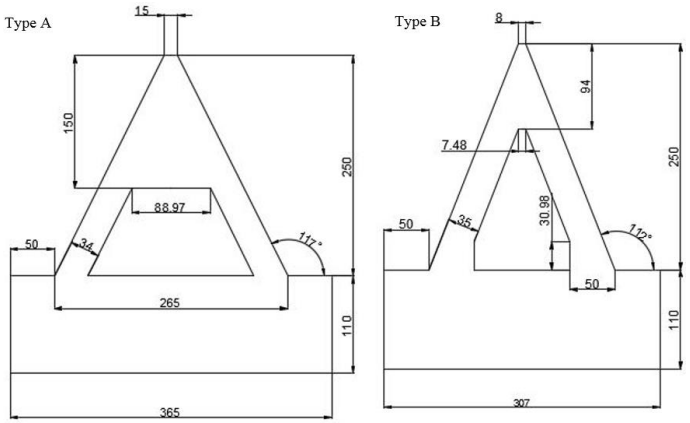

Fig. 6 The geometrical characteristics of large-scale models. For type A, t_M=2 mm and Λ_s=2500. For type B, t_M=1 mm and Λ_s=1250. All dimensions are in mm

As it has been mentioned above, the geometry of V-shaped cantilevers used in [14] (see Fig. 3a and Fig. 5) differ from the geometry of commercial V-shaped cantilevers (see Fig. 4 and Fig. 6). Further, one can see from Fig. 5 that the experimental scheme used in [14] was based on the load (torque) transfer from a clamp to the beam through a strip of the beam material where the camp is contacting with the beam. In practice, the load is transferred to the beam trough the base of the pyramidal tip as it can be seen in Fig. 1. This feature of AFM loading has been taken into account in the experiments described below.

B. Design of rectangular and V-shaped cantilevers with equal normal spring constants K_z

We needed to work with scaled-up models of rectangular and V-shape cantilevers having equal normal spring constant, length and thickness. The experimental methodology followed to achieve this started with the preparation of the large-scale V-shaped cantilever models of types A and B. The models were cut from polycarbonate sheets with thickness values t_M of 1, 2 and 3 mm. The geometry of the models was described earlier. A water jet machine was used to cut the cantilever profiles from blank polycarbonate sheets. The vertical spring constants of the manufactured models were estimated first using quasi-static deflection measurements. During each test, the cantilever was clamped at its fixed end (Fig. 7). The normal load was applied at the center of the base of the probe tip and it was increased gradually. The results obtained are shown in Fig. 8 where it is clearly seen that a linear relationship exists between the vertical deflection of the cantilever and the applied force. To determine the normal spring constant of the scaled-up cantilever models, the slope of the straight line fitted to these results was calculated. The obtained values of the normal spring constants for the V-shaped cantilevers are given in Table 1.

Next, to design rectangular cantilevers with normal spring constants K_z that were equal to the corresponding constants of the V-shaped cantilevers, the elastic modulus of the polycarbonate models was determined via an additional experiment. In this experiment, the vertical spring constant of a rectangular cantilever of some length L_0, width w_0 and thickness t_0 was measured. Using the linear approximation of the plot of the vertical force measured as a function of the

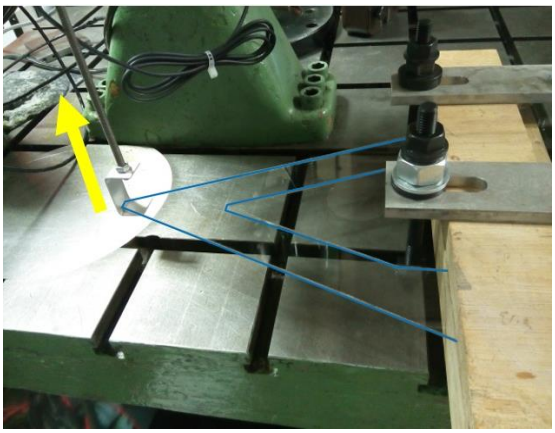

Fig. 7 An example of a large-scale model of a V-shaped cantilever subjected to normal loading. The arrows show the direction of the applied external load.

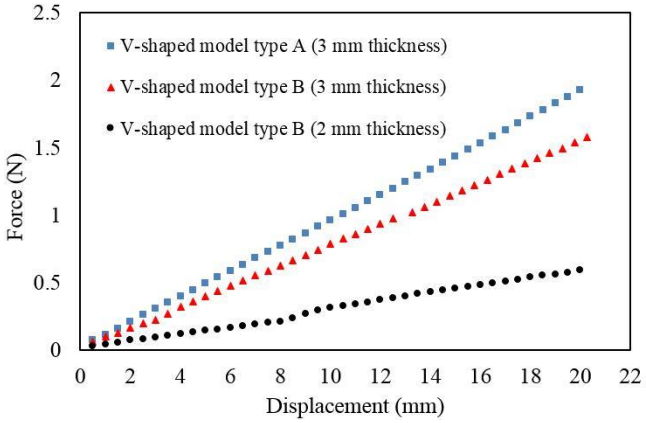

Fig. 8 The plot of the vertical force as a function of the vertical deflection for V-shaped large-scale experimental models.

vertical deflection for this rectangular, it was found that K_z=0.0292 N/m. Next, by substituting the geometrical dimensions of the rectangular cantilever used, i.e. L_0=230 mm, w_0 =70 mm, t_0=2 mm, and the value K_z =0.0292 N/mm into (3a), the elastic modulus E of the polycarbonate sheets could be evaluated as 2.538 GPa. This value was in a good agreement with the data found in the literature [37-38] for polycarbonate material as its elastic modulus generally varies from 2.5 to 3.0 GPa. Knowing this, the width, w_M, of the necessary scaled-up rectangular cantilever models could then be calculated using (3a). The values obtained are shown in Table 2. Finally, a FEM analysis was also performed to verify the validity of the above described experimental procedure. A commercial finite element package, i.e. Abaqus, was employed. The length of the rectangular cantilever was set to 250 mm, identically to the scaled-up V-shaped cantilever length (Fig. 6). The values used for the cantilever width and thickness were those shown in Table 2. The material model used was linear elastic and its elastic modulus was about 2.5 GPa. The applied vertical load used in the simulations was 2.0 N. One can calculate the corresponding K_z value for each modelled rectangular cantilever based on the simulated deflection. As shown in Table 2, a good agreement was observed between the values obtained by FEM and the initial values of the spring constants for the designed scaled-up V-shaped models.

In this way, we prepared a set of V-shaped and the corresponding rectangular cantilever samples with identical length, thickness and normal spring constants. In addition, the positions of external load application to these large-scale model samples were designed to be the same for both sets. The points of the external load application were located using arguments

TABLE I
THE EXPERIMENTAL VALUES OF THE NORMAL SPRING CONSTANT K_z FOR THE SET OF V-SHAPED CANTILEVER MODELS USED

Thickness t_M (mm)	Type	K_z (N/mm)
3	A	0.0961
3	B	0.0780
2	B	0.0302

TABLE II
THE K_z VALUES OBTAINED EXPERIMENTALLY FOR V-SHAPED CANTILEVERS, THE WIDTHS w_M OF THE CORRESPONDING RECTANGULAR CANTILEVERS AND THE K_z VALUES OBTAINED BY FEM SIMULATIONS OF THE CORRESPONDING RECTANGULAR CANTILEVERS

Cantilever thickness	Type	Experimental K_z for the V-shaped models	w_M of the corresponding rectangular cantilever	Numerical K_z of rectangular cantilevers
3 mm	A	0.0961 N/mm	69 mm	0.0972 N/mm
3 mm	B	0.0780 N/mm	56 mm	0.0787 N/mm
2 mm	B	0.0302 N/mm	73 mm	0.0305 N/mm

of the geometrical similarity to real AFM probes.

IV. EXPERIMENTAL AND NUMERICAL COMPARISON OF TORSIONAL SPRING CONSTANTS FOR EQUIVALENT RECTANGULAR AND V-SHAPE CANTILEVERS

It is known (see e.g. Sader and Sader [14]) that the lateral resistance of a cantilever is defined as the ratio K_y/K_z. Hence, if the K_z values are the same for two cantilevers of different geometry then, we just need to compare their lateral spring constants K_y. Thus, we did not use the values of the torsional deflection angle $\Delta\theta$ and the torque T in our experimental studies and numerical simulations. Instead, we estimated the lateral displacements Δy of the tip apex under the action of the force applied at the contact point. The estimation of the lateral displacements Δy allows us to compare the lateral spring constants of the rectangular and V-shaped cantilevers and, therefore their lateral resistance. As discussed earlier in section 2, one can easily calculate the torsional spring constant K_θ from the value of the lateral spring constant K_y and thus, it is the same to compare K_θ or K_y of cantilevers to analyse their susceptibility to lateral forces.

A. *Geometry of the probe tip*

As mentioned, the load transfer scheme is important for modelling the torsion of AFM cantilever beams. The external lateral load (the frictional force) is applied to an AFM probe at the apex of the imaging tip (see Fig. 1). In turn, this load is transferred to the cantilever through the base of the tip. Hence, formally one needs to apply the frictional force (F_F) to the free end of the pyramidal tip. However, the experimental realisation of this procedure using a conventional testing machine equipped with a load cell is difficult in practice because the force applied slides away from the apex of the pyramid. To avoid sliding during the application of the lateral force, we designed the following experimental procedure: the pyramidal tip is replaced by a rectangular prism whose height and base are the same as the height and the base of the pyramid. To show that this experimental scheme does not change the load transfer scheme, FEM simulations were employed. Both pyramidal and prismatic tips were loaded by a lateral force applied at the same height as shown in Fig. 9. Because the plane of the cantilevers was oriented vertically in our experimental scheme (see Fig. 10), the gravity could influence the results only by creating an additional torque due to the weight of the attached tip. However, this torque changed only the origin of the measurements and it did not affect the results. Thus, gravity has not been taken into account in the FEM model.

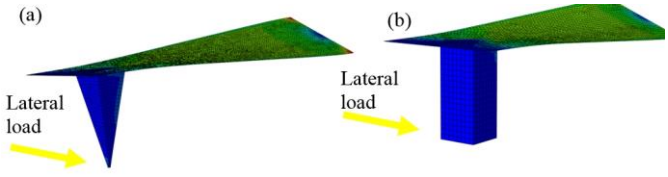

Fig. 9 The FEM models used in simulations of lateral displacement of (a) pyramidal and (b) prismatic tips attached to a rectangular cantilever.

In our experiments, the dimensions of the tip base and the tip height were taken in such way that they satisfied the above described conditions of geometrical similarity to the tips of the commercial probes. The results of our FEM simulations showed that (i) the numerically calculated lateral deflections were linear functions of the applied force and (ii) the difference between the corresponding torsional spring constants was less than 0.02%. Thus, instead of a pyramidal tip, a rectangular prismatic tip made of polycarbonate with a square base of dimensions 22 mm x 22 mm and a height h_p=54 mm was used in our experimental studies.

B. *Experimental comparison of the lateral spring constant for rectangular and V-shaped cantilevers*

After checking the validity of employing prismatic tips, we can use the experimental and numerical schemes that avoid the problems caused by the singularity of pyramidal tips at their free ends. In the experimental studies, both rectangular and V-shape cantilevers were subjected to lateral forces applied at the tip base, as shown in Fig. 10. The load was applied to a ring connected to the end of a prismatic probe. As indicated in the figure, this load was oriented in such a way that the ring was pulled-up. This resulted in a torque that was equal to the torque caused by the frictional force acting at the tip of a pyramidal probe. The experimentally measured lateral displacements of the free end of the prismatic tip attached to the cantilevers and the corresponding applied loads are plotted in Fig. 11 for the sets of scaled-up cantilever models that were fabricated in this study. It can be seen from this figure that the relationship between both physical quantities is always linear, as expected. In this figure, the applied load is given as a function of the lateral displacement such that the comparison of the lateral spring constant between equivalent V-shaped and rectangular cantilever models can be easily visualized. In this way, it is observed graphically that the lateral spring constant of a V-shaped cantilever was always higher than that of the equivalent rectangular cantilever.

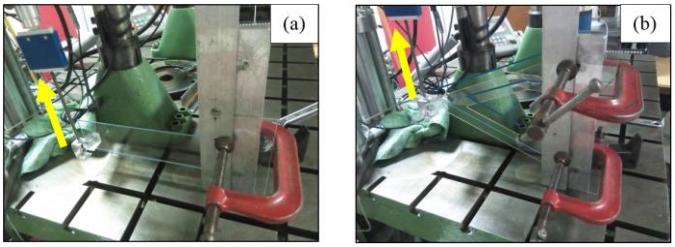

Fig. 10 The large scale (a) rectangular and (b) V-shaped models of cantilevers subjected to the lateral load transferred through a prismatic tip.

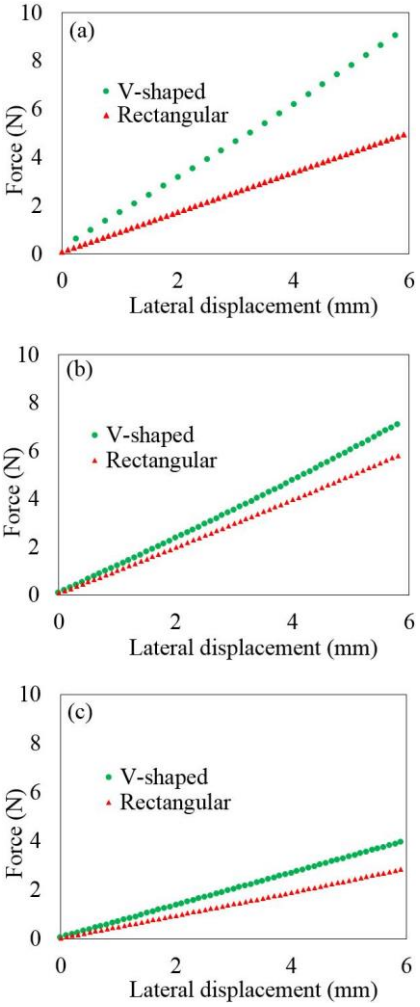

Fig. 11 Plots of measured lateral force against lateral displacement for V-shaped and rectangular cantilevers with normal spring constant: (a) K_z= 0.0780 N/mm; (b) K_z= 0.0961 N/mm; (c) K_z= 0.0302 N/mm.

C. Numerical FEM simulations of the laterally loaded AFM cantilevers

The purpose of the numerical simulations was to further compare the lateral spring constants of the rectangular and V-shaped cantilevers using FEM models. These models were prepared in accordance with the scaled-up samples used in the above-described experiments. Fig. 12 illustrates the simulated deformations of such models for two designs with different K_z values. The results of the FEM numerical simulations and the comparison between V-shaped and rectangular cantilevers are now discussed in the next section.

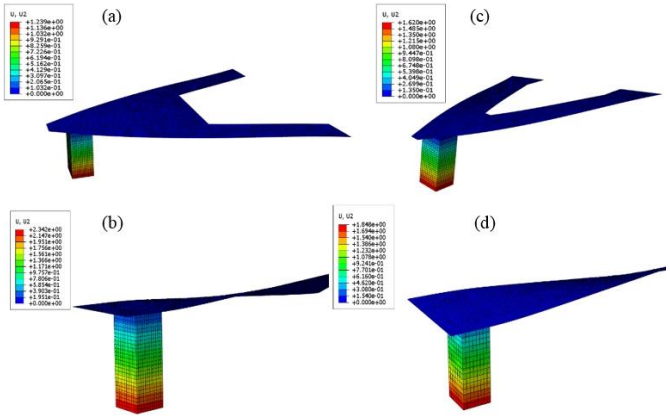

Fig. 12 FEM models used in the simulations of the lateral displacement of a prismatic tip attached to (a) V-shaped and (b) rectangular cantilevers having K_z = 0.0780 N/mm; (c) V-shaped and (d) rectangular cantilevers having K_z = 0.096 N/mm.

D. Discussion

The experimental and numerically obtained plots of the lateral load against the lateral displacement were used to extract the value of lateral spring constants for the different designs considered in this study. These values are reported in Table 3. One can see from this table, that the spring constants K_y of the V-shaped cantilevers, whose shapes were geometrically similar to the shapes of the commercially manufactured probes and loaded at the free end of the tip, are higher than the K_y values of the corresponding rectangular beams. In addition, the K_y values of V-shaped and rectangular cantilevers obtained by FEM are generally in good agreement with the experimental estimations.

It has to be pointed out that, in experiments for normal bending, cantilever samples having t_M=1 mm could experience a considerable initial deflection due to gravity and the force-displacement relations could be non-linear. Hence, these samples did not reflect the real work of AFM cantilevers and we do not present here the experimental results obtained for the samples with t_M=1 mm. Based on the experimental data reported in Table 3, it was calculated that the V-shaped cantilever of type A, with t_M=3 mm, had a lateral spring constant 15% higher than that of the rectangular cantilever. It should be noted that together with this increase of the lateral spring constant, the volume, and hence the mass, of this V-shaped cantilever is greater than that of the corresponding rectangular cantilever by 8.6%. On the other hand, there was a 46% increase in the experimentally assessed lateral spring constant for the V-shaped cantilever of type B, with t_M=3 mm, in comparison with the constant of the rectangular beam. Note

TABLE III
EXPERIMENTAL AND NUMERICAL VALUES OF THE LATERAL SPRING CONSTANT K_y FOR EQUIVALENT V-SHAPED AND RECTANGULAR CANTILEVERS

Cantilever thickness	Type	V-shaped K_y (N/mm)		Rectangular K_y (N/mm)		Percentage difference in the experimental value of K_y between V-shaped and rectangular cantilevers
		Experiments	FEM	Experiments	FEM	
3 mm	A	1.20	1.23	0.99	1.08	18%
3 mm	B	1.54	1.61	0.83	0.85	46%
2 mm	B	0.66	0.49	0.47	0.43	29%

that the volume of this cantilever was 25.6% higher than the volume of the corresponding rectangular beam.

V. Conclusions

The properties of force-sensing micro-cantilevers are of fundamental importance for measurements employing atomic force microscopy (AFM) techniques. Here, we focus on AFM applications involving lateral forces. There are various areas where the lateral mode of AFM is very important, e.g. manipulation of very small objects or nanotribology tests when an AFM works as a frictional force microscope (FFM). The present study was induced by the well-known statement [13,14] that is generally accepted in the nanotechnology community: V-shaped AFM cantilevers offer less resistance to lateral forces than rectangular cantilevers. We have shown that this statement is not true in application to cantilevers fabricated by an AFM probe manufacturer. This conclusion is based on results of numerical (finite element modelling) and experimental comparisons between the torsional spring constants of rectangular and V-shaped AFM cantilevers that were made of the same material and that have the same length, thickness, normal spring constant, as well as the location and the shape of the tip base. In particular, it has been shown that the torsional spring constant of the considered commercial V-shaped cantilever samples can be greater than the constant of a corresponding rectangular beam by up to 45% depending on the specific geometry of the cantilever. Because the V-shaped probes manufactured by Olympus, NanoWorld and other AFM probe manufacturers are quite similar, we took probes from the Olympus company as a representative sample of commercial V-shaped cantilevers, namely the cantilevers of the OMCL-TR series. We argue that the results of the experiments described in [14] do not necessarily apply for the interpretation of the operations of all commercial AFM cantilevers. This discrepancy of outcome with the present study should be caused by differences in the load transfer scheme and the geometrical shapes of the used V-shaped models.

Acknowledgments

Dr Raheem S.J. Al-Musawi would like to thank the Iraqi Ministry of Higher Education and Scientific Research (MOHESR) and Kufa University, Department of Mechanical Engineering in Iraq for the financial support provided. F.M. Borodich has been involved in the studies within the CARBTRIB International Network; he is grateful to the Leverhulme Trust for the financial support of the network.

References

[1] G. Binnig, C. F. Quate and C. Gerber, "Atomic force microscope," *Phys. Rev. Lett.,* vol. 56, pp. 930-933, 1986.

[2] M. A. Sánchez Quintanilla, "Surface analysis using contact mode AFM" in *Encyclopedia of Tribology* ed Q. J. Wang and Y.-W. Chung, Springer, Boston, MA, vol. 2, pp. 3401-3411, 2013.

[3] A. Podestá, "Surface analysis using dynamic AFM" in *Encyclopedia of Tribology* ed Q. J .Wang and Y.-W. Chung, Springer, Boston, MA, vol. 2, pp. 3411-3418, 2013.

[4] F. M. Borodich, A. Pepelyshev and O. Savencu, "Statistical approaches to description of rough engineering surfaces at nano and microscales," *Tribol. Int.*, vol. 103, pp197-207, 2016.

[5] C. M. Mate, G. M. McClelland, R. Erlandsson and S. Chiang, "Atomic-scale friction of a tungsten tip on a graphite surface," *Phys. Rev. Lett.*, vol. 59, pp. 1942-1945, 1987.

[6] D. F. Ogletree, R. W. Carpick and M. Salmeron, "Calibration of frictional forces in atomic force microscopy," *Rev. Sci. Instrum.*, vol. 67, pp. 3298-3306, 1996.

[7] R. S. J. Al-Musawi, E. B. Brousseau, Y. Geng and F. M. Borodich, "Insight into mechanics of AFM tip-based nanomachining: bending of cantilevers and machined grooves," *Nanotechnology*, vol. 27, pp. 385302-385316, 2016.

[8] X. Chen, S. Zhang, D. A. Dikin, W. Ding, R. S. Ruoff, L. Pan and Y. Nakayama, "Mechanics of a carbon nanocoil," *Nano Lett.*, vol. 3, pp. 1299-1304, 2003.

[9] M. H. Korayem and M. Zakeri, "The effect of off-end tip distance on the nanomanipulation based on rectangular and V-shape cantilevered AFMs," *Int. J. Adv. Manuf. Technol.*, vol 50, pp. 579-589, 2010.

[10] E. C. Preedy, S. Perni, and P. Prokopovich, "Nanomechanical and surface properties of rMSCs post exposure to CAP treated UHMWPE wear particles," *Nanomedicine: Nanotechnology, Biology and Medicine*, vol. 12, pp. 723-734, 2016.

[11] I. Acerbi, T. Luque, A. Giménez, M. Puig, N. Reguart, R. Farré, D. Navajas and J. Alcaraz, "Integrin-specific mechanoresponses to compression and extension probed by cylindrical flat-ended AFM tips in lung cells," *PLoS One*, vol. 7, e32261, 2012.

[12] A. Yacoot and L. Koenders, "Aspects of scanning force microscope probes and their effects on dimensional measurement," *J. Phys. D: Appl. Phys.*, vol. 41, 103001, 2008.

[13] J. E. Sader, "Susceptibility of atomic force microscope cantilevers to lateral forces," *Rev. Sci. Instrum.*, vol. 74, no. 4, pp. 2438-2443, 2003.

[14] J. E. Sader and R. C. Sader, "Susceptibility of atomic force microscope cantilevers to lateral forces: Experimental verification," *Appl. Phys. Lett.*, vol. 83, no. 15, pp. 3195-3197, 2003.

[15] J. M. Neumeister and W. A. Ducker, "Lateral, normal, and longitudinal spring constants of atomic force microscopy cantilevers," *Rev. Sci. Instrum.*, vol. 65, no. 8, pp. 2527-2531, 1994.

[16] M. Varenberg, I. Etsion and G. Halperin, "An improved wedge calibration method for lateral force in atomic force microscopy," *Rev. Sci. Instrum.*, vol. 74, no. 7, pp. 3362-3367, 2003.

[17] S. Timoshenko, in *Strength of Materials. Part 1. Elementary Theory and Problems*, 2nd ed., New York, USA: D. Van Nostrand Company, 1940.

[18] D. Sarid, in *Scanning force microscopy: with applications to electric, magnetic and atomic forces*, Oxford University Press, New York, USA, p. 5, 1994.

[19] B. Bhushan and O. Marti "Scanning probe microscopy - principle of operation, instrumentation, and probes" in *Handbook of Nanotechnology*, ed Bhushan B., Springer-Verlag Berlin Heidelberg, 3rd ed., pp. 573-617, 2010.

[20] H.-J. Butt, B. Capella and M. Kappl, "Force measurements with the atomic force microscope: Technique, interpretation and applications," *Surf. Sci. Rep.*, vol. 59, pp. 1-152, 2005.

[21] L.-O. Heim, M. Kappl and H.-J. Butt, "Tilt of atomic force microscope cantilevers: effect on spring constant and adhesion measurements," *Langmuir*, vol. 20, no. 7, pp. 2760-2764, 2004.

[22] J. L. Hutter, "Comment on tilt of atomic force microscope cantilevers: effect on spring constant and adhesion measurements," *Langmuir*, vol. 21, no. 6, pp. 2630-2632, 2005.

[23] J. D. Holbery, V. L. Eden, M. Sarikaya and R. M. Fisher, "Experimental determination of scanning probe microscope cantilever spring constants utilizing a nanoindentation apparatus," *Rev. Sci. Instrum.*, vol. 71, no. 10, pp. 3769-3776, 2000.

[24] C. A. Clifford and M. P. Seah, "The determination of atomic force microscope cantilever spring constants via dimensional methods for nanomechanical analysis," *Nanotechnology*, vol. 16, no. 9, pp. 1666-1680, 2005.

[25] R. J. Cannara, M. Eglin and R. W. Carpick, "Lateral force calibration in atomic force microscopy: A new lateral force calibration method and general guidelines for optimization," *Rev. Sci. Instrum.*, vol. 77, no. 5, 053701, 2006.

[26] T. R. Albrecht and C. F. Quate, "Atomic resolution imaging of a nonconductor by atomic force microscopy," *J. Appl. Phys.*, vol. 62., no. 7, pp. 2599-2602, 1987.

[27] T. R. Albrecht, S. Akamine, T. E. Carver and C. F. Quate, "Microfabrication of cantilever styli for the atomic force microscope," *J. Vac. Sci. Technol. A*, vol. 8, no. 4, pp. 3386-3396, 1990.

[28] D. R. Baselt and J. D. Baldeschwieler, "Lateral forces during atomic force microscopy of graphite in air," *J. Vac. Sci. Technol. B*, vol. 10, no. 5, pp. 2316-2322, 1992.
[29] Green C. P., Lioe H., Cleveland J. P., Proksch R., Mulvaney P. and Sader J. E. "Normal and torsional spring constants of atomic force microscope cantilevers," *Rev. Sci. Instrum.*, vol. 75, no. 6, pp. 1988-1996, 2004.
[30] J. L. Hazel and V. V. Tsukruk, "Friction force microscopy measurements: Normal and torsional spring constants for V-shaped cantilevers," *J. Tribol.*, vol. 120, no. 4, pp. 814-819, 1998.
[31] R. Álvarez-Asencio, E. Thormann and M. W. Rutland, "Determination of torsional spring constant of atomic force microscopy cantilevers: combining normal spring constant and classical beam theory." *Rev Sci Instrum.*, vol. 84, no. 9, 096102 , 2013.
[32] J. D. Parkin and G. Hähner, "Calibration of the torsional and lateral spring constants of cantilever sensors," *Nanotechnology*, vol. 25, no. 22, 225701, 2014.
[33] A. H. Korayem, A. K. Hoshiar, S. Badrlou and M. H. Korayem, "A comprehensive model for stiffness coefficients in V-shaped cantilevers," *Int. J. Nanosci. Nanotechnol.*, vol. 12, no. 1, pp. 27-36, 2016.
[34] Olympus Micro cantilever (2012) http://probe.olympus-global.com/image/support/dl/insg/probe/catalog/MEMS15E_Jul2012.pdf
[35] Barenblatt G. I., in *Scaling*, Cambridge, UK: Cambridge University Press, 2003.
[36] B. N. Ushakov and I. P. Frolov, in *Stresses in Composite Constructions*, Moscow: Mashinovedenie (in Russian) 1979.
[37] E. R. Parker, in *Materials Data Book for Engineers and Scientists*, New York: McGraw-Hill, 1967.
[38] S. Kalpakjian and S. R. Schmid, in *Manufacturing Processes for Engineering Materials*, Upper Saddle River: Pearson Education, 2008.